Online Resource 5

Title: Parameters of the dynamic model: Human & Exoskeleton.

Description: The characteristic parameters of the human–exoskeleton system include segment lengths and masses, the positions of the COMS of each segment, and their corresponding moments of inertia. Some of these parameters change across the gait cycle phases, as the mass distribution of the segments changes during movement. Accordingly, this supplementary material presents the parameter sets of the RUVEM and Exo-H3 exoskeletons, together with the anthropometric parameters of the human model derived from a virtual mannequin.

Article: Dynamic modeling of human–exoskeleton interaction: A simulation framework for gait rehabilitation.

Journal: Multibody System Dynamics

Authors: Sergey González-Mejía and José Miguel Ramírez-Scarpetta

Corresponding author: Universidad del Valle, sergey.gonzalez@correounivalle.edu.co

Parameters of the dynamic model:

Human & Exoskeleton

Contents

Parameters of the dynamic model: Human & Exoskeleton **1**

1. Case study: RUVEM exoskeleton **1**

1.1 RUVEM Lower limb exoskeleton 2
1.2 Virtual mannequin 9
1.3 Mannequin + RUVEM exoskeleton 16
1.4 RUVEM Actuator 23

2. Case study: Exo-H3 exoskeleton **24**

2.1 Exo-H3 Lower limb exoskeleton 25
2.2 Exo-H3 Actuator 27

3. References **28**

Parameters of the dynamic model: Human & Exoskeleton

The characteristic parameters of the human–exoskeleton system include segment lengths and masses, the positions of the COMS of each segment, and their corresponding moments of inertia. Some of these parameters change across the gait cycle phases, as the mass distribution of the segments changes during movement [1]. Accordingly, this supplementary material presents the parameter sets of the RUVEM and Exo-H3 exoskeletons, together with the anthropometric parameters of the human model derived from a virtual mannequin.

1. Case study: RUVEM exoskeleton

The RUVEM exoskeleton, Fig. 1(a), and the virtual mannequin, Fig. 1(b), are designed under Catia/Delmia V5.0 software [2, 3], where the mannequin is rigidly coupled to a lower limb exoskeleton that has motors in the knee and hip joints, Fig. 1(c). The virtual mannequin design consists of anthropometric parameters that define the size and geometric shape of the body segments where the design uses data reported in [4], and the mannequin can be parameterized in height and total mass. Concerning the respective simulations, a subject with an anthropometric height of 1.77 m and a weight of 72 Kg is considered. The origin of the coordinate frame shifts with the supporting limb between 50% and 60% of the gait cycle, as illustrated in Fig. 1(e). The Catia/Delmia simulation remains static, analyzing only the evolution of the COM positions and the moments of inertia.

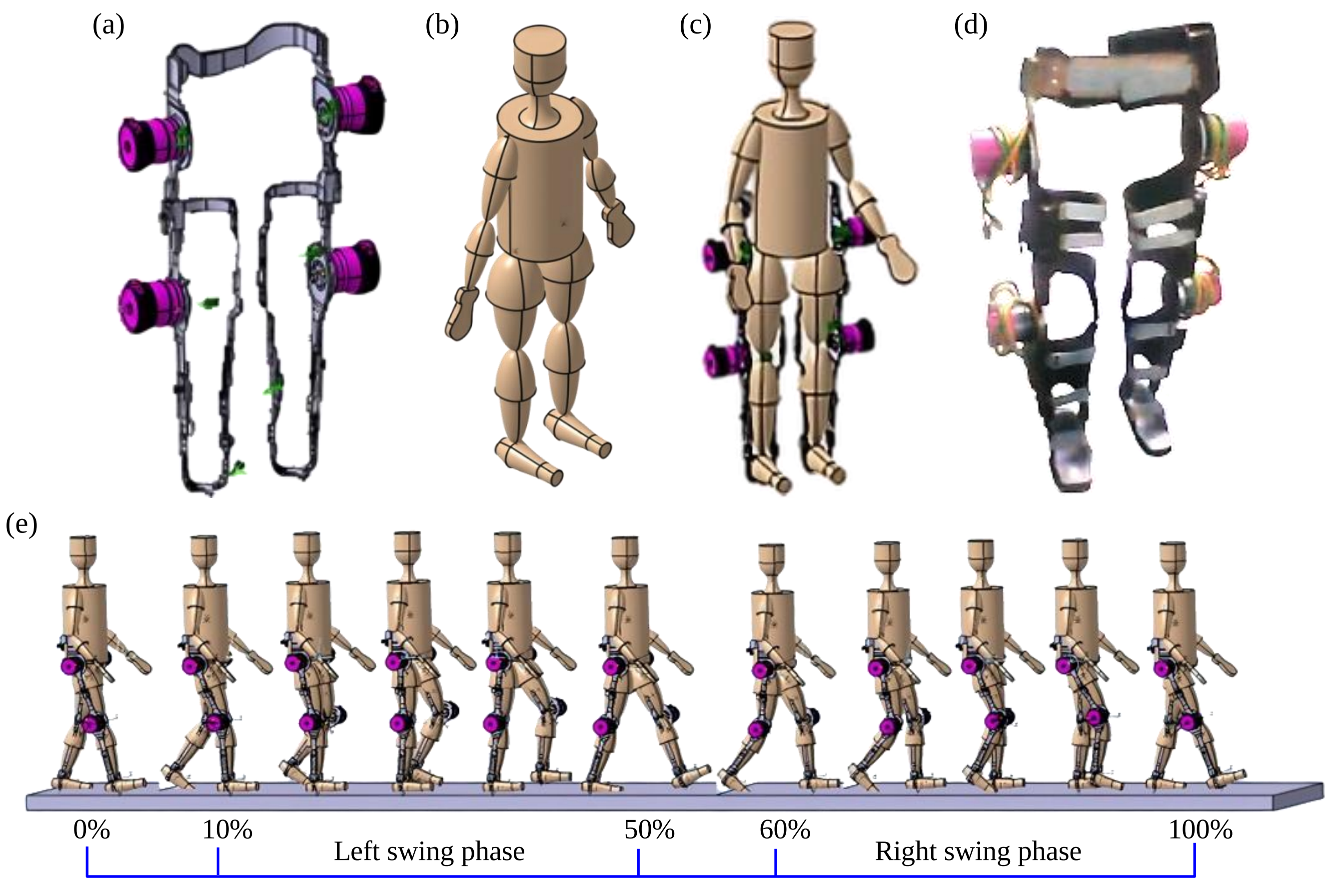

Fig. 1 RUVEM lower limb exoskeleton. (a) CAD model for RUVEM exoskeleton, (b) Virtual mannequin, (c) Virtual mannequin-RUVEM exoskeleton, (d) RUVEM exoskeleton owned by GICI group [5], and (e) Simulation of Mannequin-RUVEM exoskeleton system under Catia/Delmia software

1.1 RUVEM Lower limb exoskeleton

This section describes the main physical parameters of the RUVEM lower limb exoskeleton, Fig. 1(d), which are essential to parameterize a reliable dynamic model of the human–exoskeleton system. The parameters include the COM positions for each lower limb segment and the corresponding moments of inertia calculated about the COMs. These values provide the necessary foundation for accurately representing the dynamic behavior of the exoskeleton during motion and for further analysis of its interaction with the human user.

- ***Positions of the COMs:*** The mass distribution in each segment changes throughout a gait cycle, therefore the COM position in the segment also changes; Table 1 lists the masses of the exoskeleton segments without motors.

Table 1 Mass of exoskeleton segments without motors

Right/left segment	**Mass** $[\boldsymbol{Kg}]$
Foot	0.184
Tibia	1.183
Femur	1.395
HAT	1.578

For the double support phase, Table 2 shows the values of the distal distances between the joints of the segments and the positions of the COMs. Also, Fig. 2 illustrates the COM positions in the right and left lower segments according to joint.

Table 2 COM's positions in the lower segments, phase: double support - RUVEM Exoskeleton with motors

Segment	**Distal distance** $[\boldsymbol{m}]$
Right foot - Ankle	0.061225
Right tibia - Ankle	0.372281
Right femur - Knee	0.387027
HAT - Right hip	0.152183
HAT - Middle hip	**0.105851**
HAT - Left hip	0.165581
Left foot - Ankle	0.062028
Left tibia - Ankle	0.373077
Left femur - Knee	0.376792

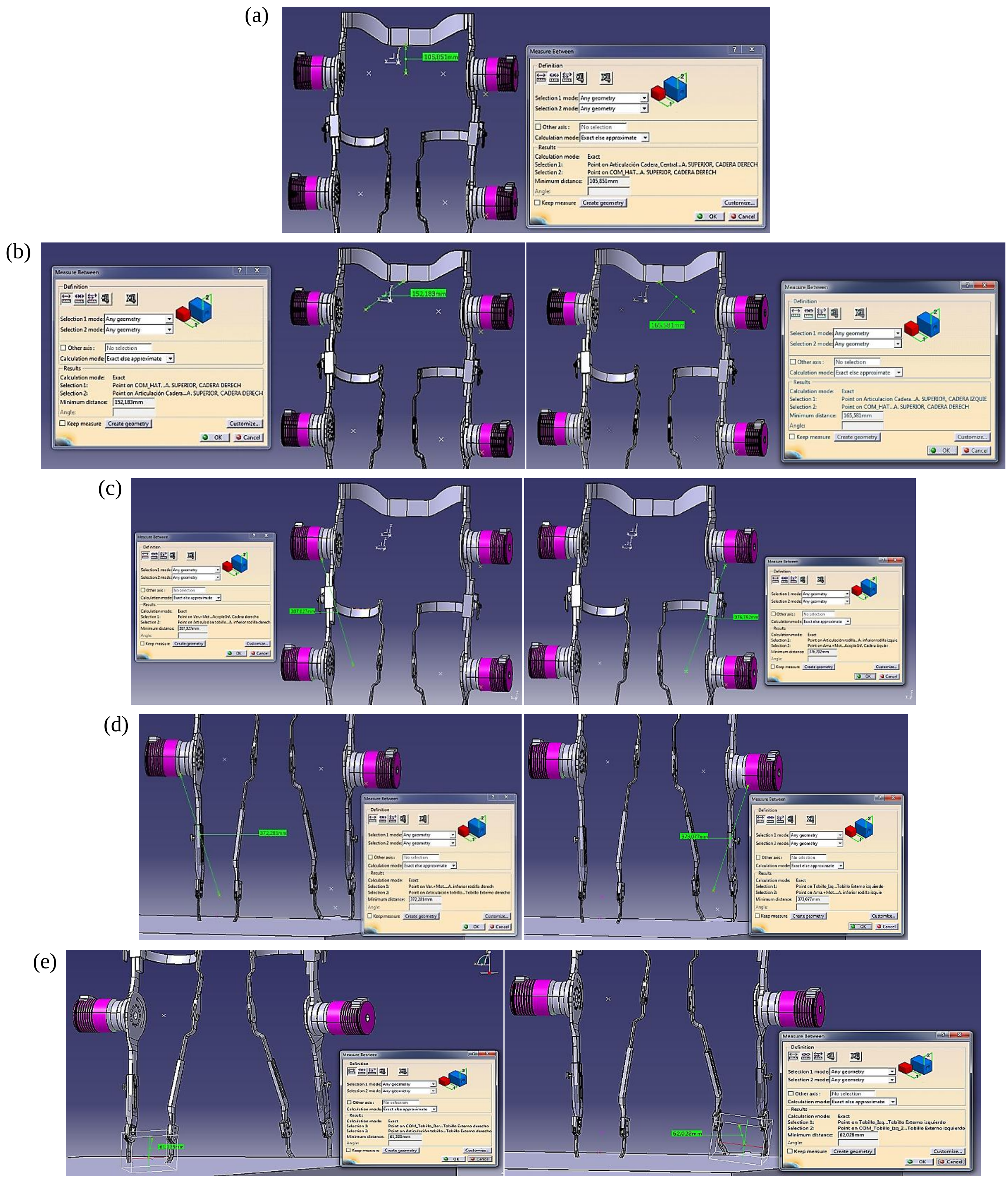

Fig. 2 COM positions in the lower limb segments during the double-support phase of the RUVEM exoskeleton: (a) Hip at the center, (b) COM position in the HAT with right and left hip, (c) COM position in the right and left femur, (d) COM position in the right and left tibia, (e) COM position in the right and left foot

For the right support and left swing phase, Fig. 3 and Table 3 show the values of the distal distances between the joints of the respective segments and the positions of the COMs. There are no changes in the segments of the right limb; It is considered in the mathematical model that the distance between any of the two hips and the COM position in the HAT is the same during the gait cycle; in addition, the proximal distance of the COM for the swing segment is used, which is calculated as the difference between the segment length and the distal distance of the COM.

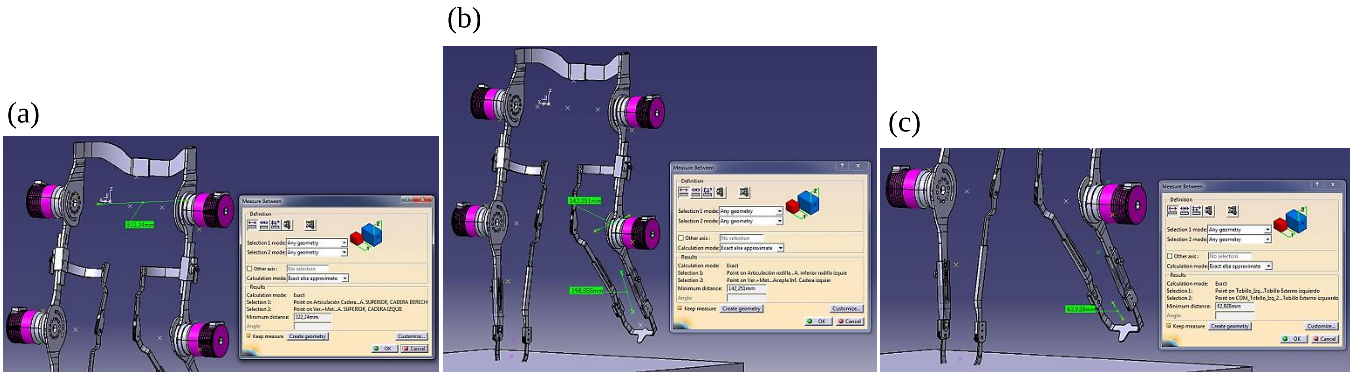

Fig. 3 COM positions in the lower segments, phase: right support/left swing - RUVEM Exoskeleton. (a) COM position in HAT - right hip in support, (b) COM position in the left tibia and left femur, both in a swing phase, and (c) COM position on left foot in the swing phase

Table 3 COM's positions in the lower segments, phase: right support and left swing - RUVEM Exoskeleton with motors

Segment	**Distal distance** $[m]$
Right foot - Ankle	0.061225
Right tibia - Ankle	0.372281
Right femur - Knee	0.387027
HAT - Right hip	**0.32224**
Left foot - Ankle	0.062028
Left tibia - Ankle	0.198855
Left femur - Knee	0.142251

The distal distances between the joints and the positions of the COMs for the left support and right swing phase are specified in Table 4 and Fig. 4. The values for the left limb segments are the same as in the double support phase.

Table 4 COM's positions in the lower segments, phase: left support and right swing - RUVEM Exoskeleton with motors

Segment	**Distal distance** $[m]$
Right foot - Ankle	0.061225
Right tibia - Ankle	0.196802
Right femur - Knee	0.142776
HAT - Left hip	**0.327531**
Left foot - Ankle	0.062028
Left tibia - Ankle	0.373077
Left femur - Knee	0.376792

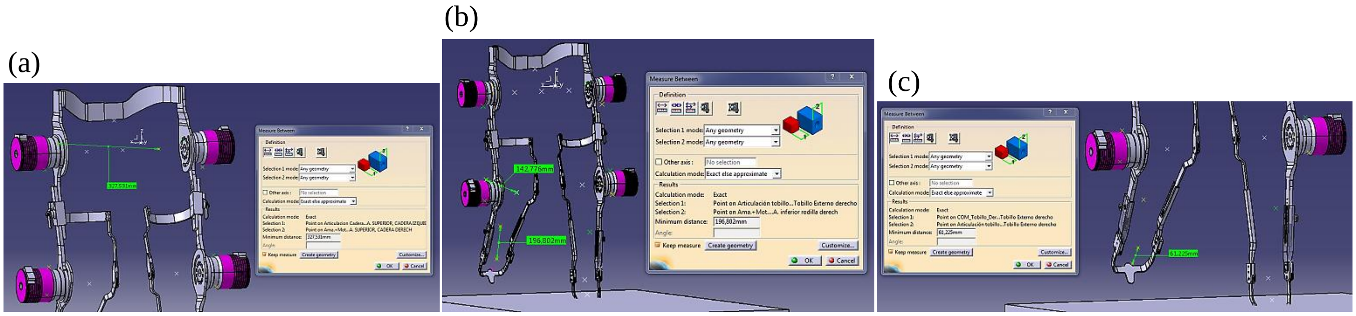

Fig. 4 COM positions in the lower segments, phase: left support and right swing - RUVEM Exoskeleton. (a) COM position in HAT - left hip in support, (b) COM position in the right tibia and right femur, both in a swing phase, and (c) COM position on right foot in the swing phase

- ***Moments of inertia:*** In each joint and segment, this parameter changes according to the current phase of the gait cycle. The moments of inertia estimated in the software package represent the tensor of inertia in a given joint; according to the reference system, the joints rotate around the $\boldsymbol{x}$-axis, $\boldsymbol{I_{oxA}}$, therefore, the parallel axes theorem [6] is used to calculate the moment of inertia parallel to the main axis and passing through the COM of the segment belonging to the joint, $\boldsymbol{I_{oxG}}$, Equation (1).

$$\begin{aligned} I_{axis\_x} &= I_{axis\_COM} + md^2 \\ I_{oxA} &= I_{oxG} + md^2 \\ I_{oxG} &= I_{oxA} - md^2 \end{aligned} \tag{1}$$

Where $I_{axis\_x} = I_{oxA}$ denote the moment of inertia about the $x -$ axis, $[Kgm^2]$, $I_{axis\_COM} = I_{oxG}$ the moment of inertia parallel to the x-axis passing through the COM of the segment, $[Kgm^2]$, m the segment mass, $[Kg]$, d the distance between the two considered parallel axes, that is, the distal distance between the articulation of the segment, and the position of the COM in the same segment, $[m]$.

For the double support phase, Table 5 lists the moments of inertia passing through the COMs of the lower segments, and Fig. 5 shows the selected lower segments in the exoskeleton, both, right and left sides, to estimate the moments of inertia.

Table 5 Moments of inertia passing through the COM of the segment with respect to the axis of rotation, phase: double support - RUVEM Exoskeleton

Joint – Segment	$\boldsymbol{I_{axis\_COM} = I_{oxG} [Kgm^2]}$
Right ankle - Right foot	0.0002692
Right ankle - Tibia	0.068
Right knee - Femur	0.064
Right hip - HAT	**0.015**
Left hip - HAT	**0.015**
Left knee- Femur	0.081
Left ankle - Tibia	0.068
Left ankle - Left foot	0.0002722

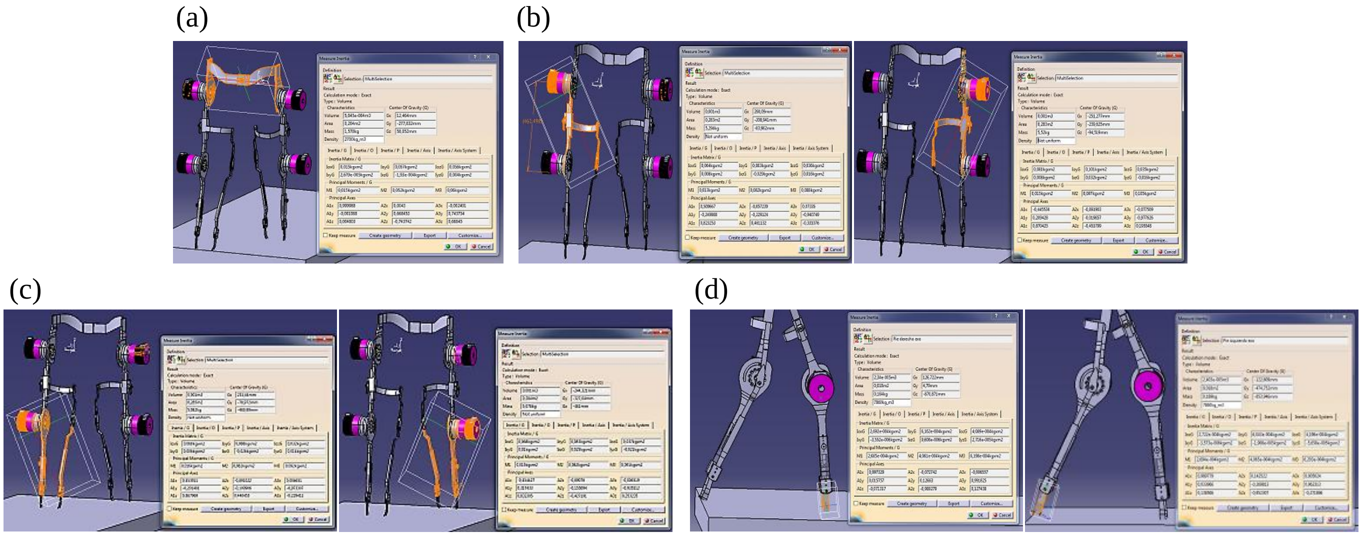

Fig. 5 Moments of inertia in the COMs of the lower segments, phase: double support - RUVEM Exoskeleton. (a) Right and left hip in support, (b) Right and left knee in support, (c) Right and left ankle in support, (d) Right and left foot in support

The moments of inertia in the COMs of the lower segments for the right support-left swing phase are detailed in Table 6 and Fig. 6. The moments of inertia of the right segments in single support are the same as in the double support phase, Fig. 5(b-d, Column 1), except for the Right hip - HAT segment, Fig. 6(a).

Table 6 Moments of inertia passing through the COM of the segment with respect to the axis of rotation, phase: right support and left swing - RUVEM Exoskeleton

Joint - Segment	$I_{axis\_COM} = I_{oxG}[Kgm^2]$
Right ankle - Right foot	0.0002692
Right ankle - Tibia	0.068
Right knee - Femur	0.064
Right hip - HAT	**0.033**
Left hip - Femur	0.07
Left knee - Tibia	0.027
Left ankle - Left foot	0.0002722

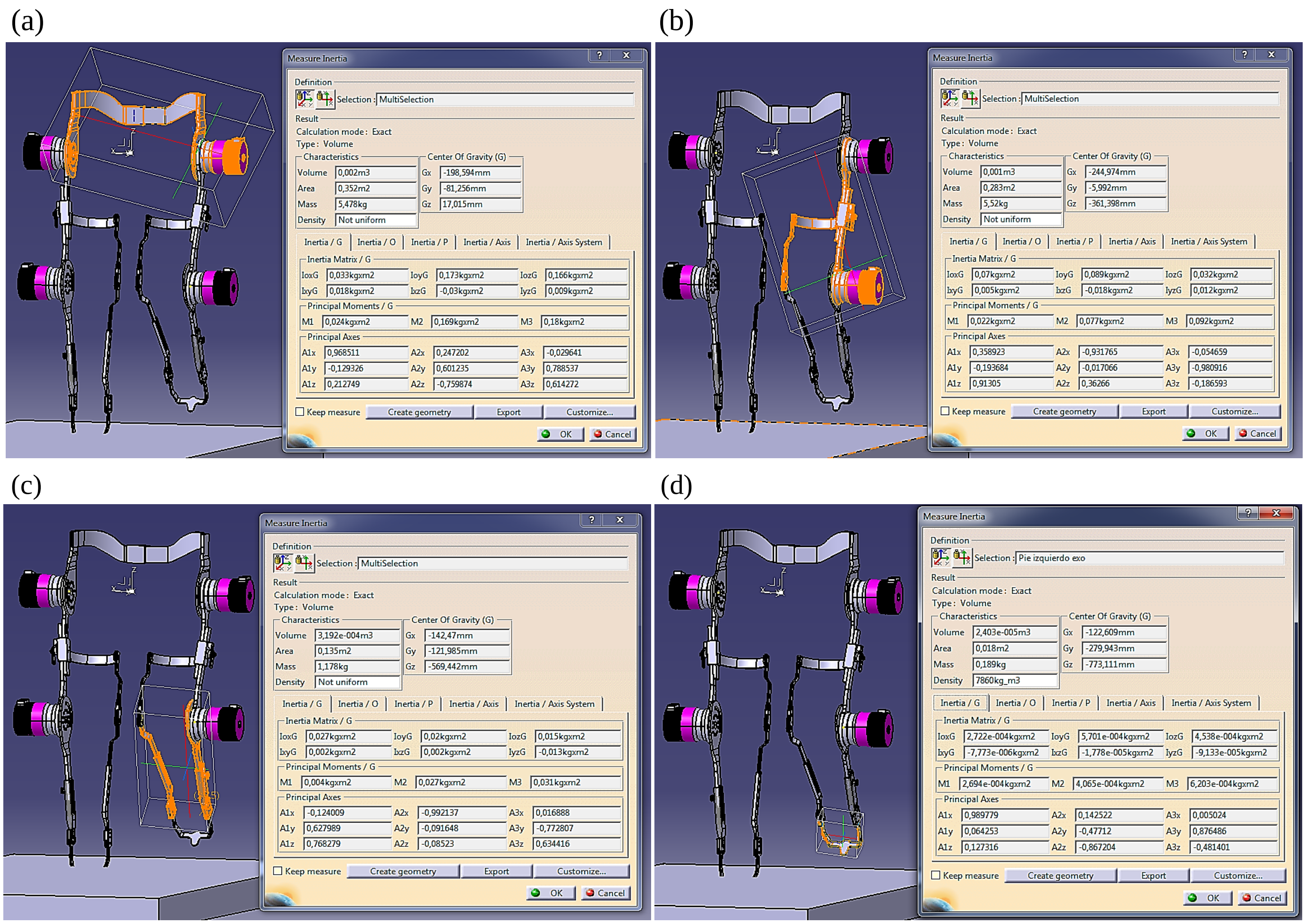

Fig. 6 Moments of inertia in the COMs of the lower segments, phase: right support and left swing - RUVEM Exoskeleton. (a) Right hip in support, (b) Left hip swing, (c) Left knee swing, and (d) Left ankle swing

The moments of inertia in the COMs of the segments for the left support-right swing phase are specified in Table 7. Similarly, the moments of inertia of the left segments in single support are the same as in the double support phase, Fig. 5(b-d, Column 2), except for the left hip - HAT segment, Fig. 7(a).

Table 7 Moments of inertia passing through the COM of the segment with respect to the axis of rotation, phase: left support and right swing - RUVEM Exoskeleton

Joint - Segment	$I_{axis\_COM} = I_{oxG}[Kgm^2]$
Right ankle - Right foot	0.0002692
Right knee - Tibia	0.027
Right hip - Femur	0.066
Left hip - HAT	**0.033**
Left knee- Femur	0.081
Left ankle - Tibia	0.068
Left ankle - Left foot	0.0002722

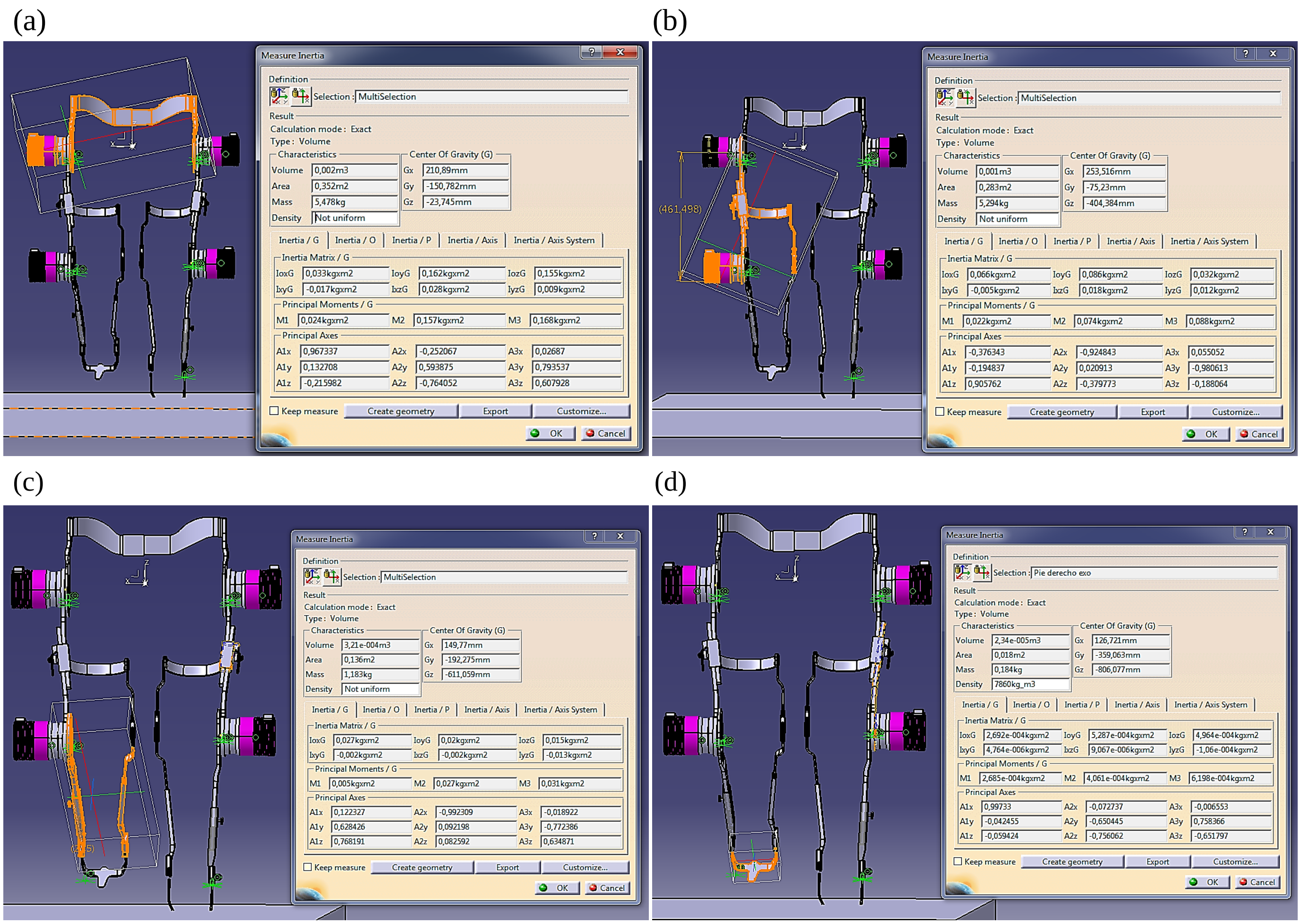

Fig. 7 Moments of inertia in the COMs of the lower segments, phase: left support and right swing - RUVEM Exoskeleton. (a) Left hip in support, (b) Right hip swing, (c) Right knee swing, (d) Right ankle swing

1.2 Virtual mannequin

This section presents the physical parameters of a virtual mannequin used to represent the human behavior in the dynamic model, Fig. 1(d). The defined parameters include the positions of the COMs for each lower limb segment, the corresponding moments of inertia about the COMs, and the lengths of the lower limb segments. These parameters enable a consistent comparison and integration with the exoskeleton model for accurate simulation of the human–exoskeleton interaction.

- ***Length of lower segments:*** The length of a segment is measured between two joints belonging to the same segment; the lengths of the lower segments on the virtual mannequin are listed in Table 8.

Table 8 Length of the lower segments on the virtual mannequin

Right/left segment	**Length** $[\boldsymbol{m}]$
Tibia	0.4182
Femur	0.4165
Foot	0.10

- ***Positions of the COMs:*** The COM position in the human segment also changes according to the phase in the gait cycle; the masses of the human segments are listed in Table 9.

Table 9 Mass of human segments

Right/left segment	**Mass** $[\boldsymbol{Kg}]$
Foot	1.046
Tibia	3.348
Femur	7.2
HAT	48.818

The distal distances for the COM positions in the double support phase are shown in Table 10, and the COM positions in the right and left lower segments can be seen in Fig. 8.

Table 10 COM's positions in the lower segments, phase: double support – virtual mannequin

Segment	**Distal distance** $[\boldsymbol{m}]$
Right foot - Ankle	0.083811
Right tibia - Ankle	0.223965
Right femur - Knee	0.235306
HAT - Right hip	0.331128
HAT - Middle hip	**0.309131**
HAT - Left hip	0.331128
Left foot - Ankle	0.083811
Left tibia - Ankle	0.223965
Left femur - Knee	0.235305

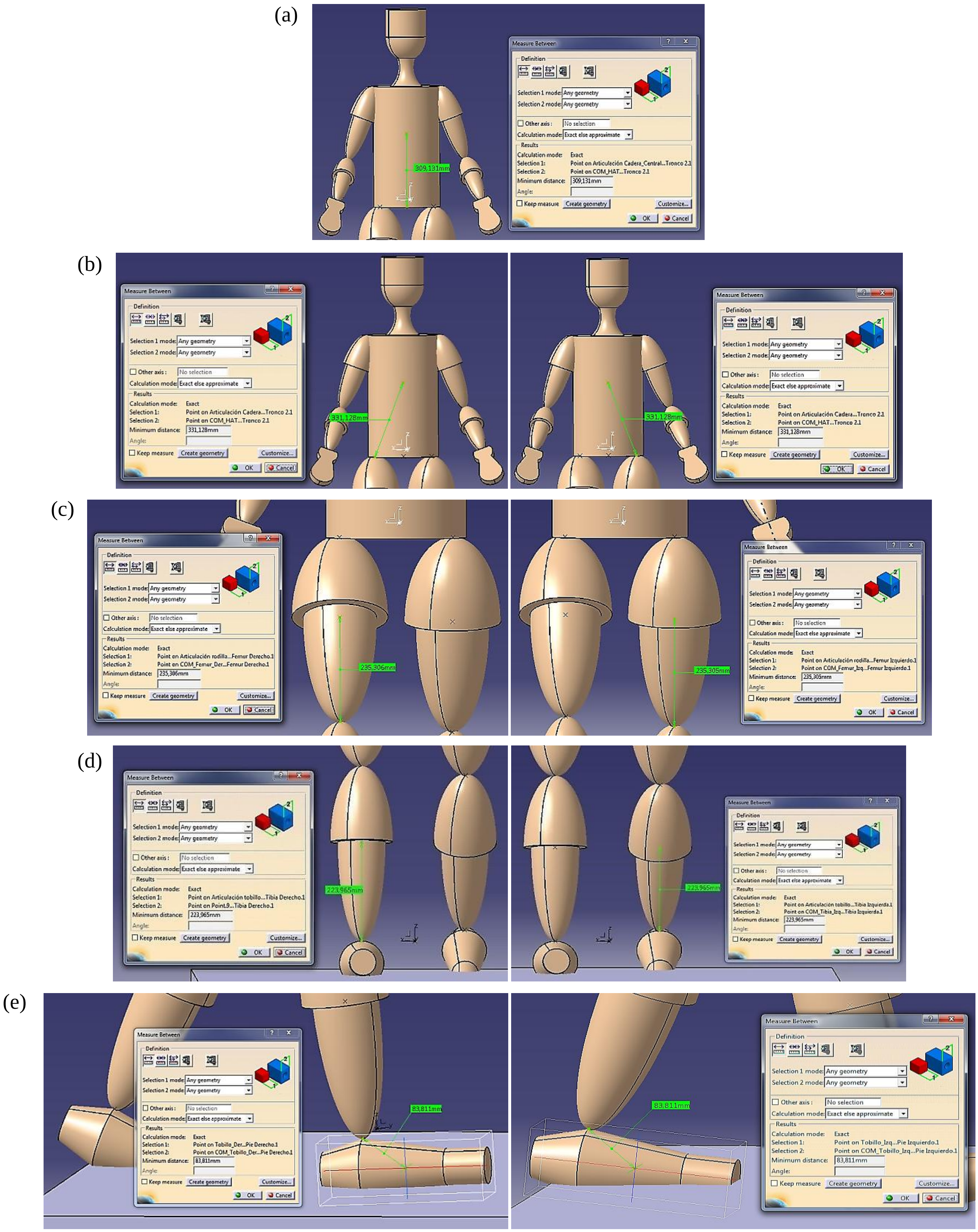

Fig. 8 COM positions in the lower limb segments during the double-support phase of the virtual mannequin: (a) Hip at the center, (b) COM position in the HAT with right and left hip, (c) COM position in the right and left femur, (d) COM position in the right and left tibia, (e) COM position in the right and left foot

For the right support and left swing phase, the distal distances between the joints and the COM positions are shown in Table 11 and Fig. 9. The same way, the proximal distance of the COM for the swing segment is used in the dynamic model.

Table 11 COM's positions in the lower segments, phase: right support and left swing – virtual mannequin

Segment	Distal distance $[m]$
Right foot - Ankle	0.083811
Right tibia - Ankle	0.223965
Right femur - Knee	0.235306
HAT - Right hip	**0.331128**
Left foot - Ankle	0.083811
Left tibia - Ankle	0.224035
Left femur - Knee	0.235305

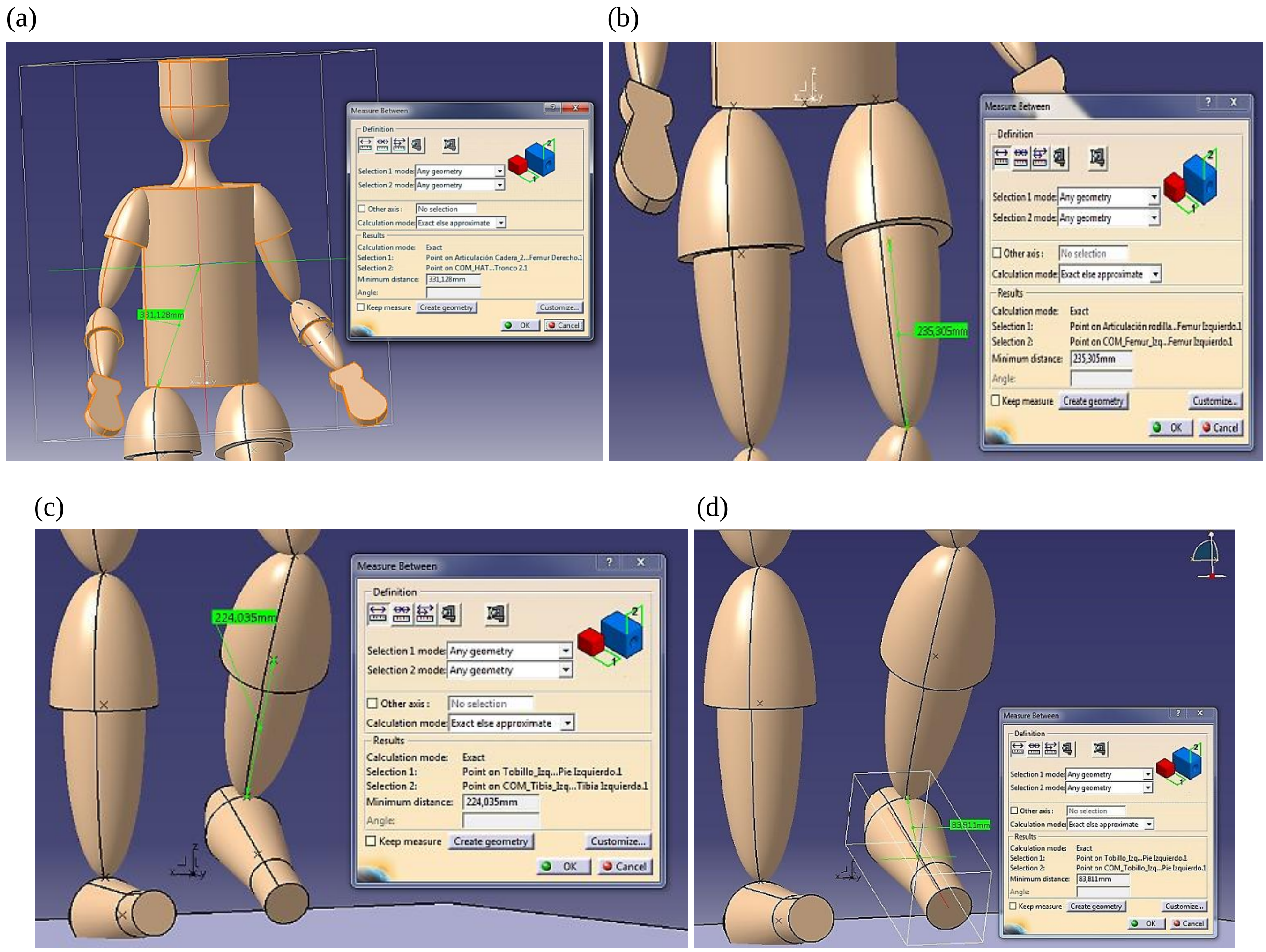

Fig. 9 COM positions in the lower segments, phase: right support and left swing – virtual mannequin. (a) COM position in HAT - right hip in support, (b) COM position in the left femur, (c) COM position in the left tibia, and (d) COM position on left foot in the swing phase

The distal distances of the COM positions for the left support-right swing phase are specify in Table 12 and Fig. 10, and the values for the left limb segments in single support phase are the same as in the double support phase, Fig. 8.

Table 12 COM's positions in the lower segments, phase: left support and right swing – virtual mannequin

Segment	Distal distance $[m]$
Right foot - Ankle	0.083811
Right tibia - Ankle	0.223965
Right femur - Knee	0.235306
HAT – Left hip	**0.331128**
Left foot - Ankle	0.083811
Left tibia - Ankle	0.223965
Left femur - Knee	0.235305

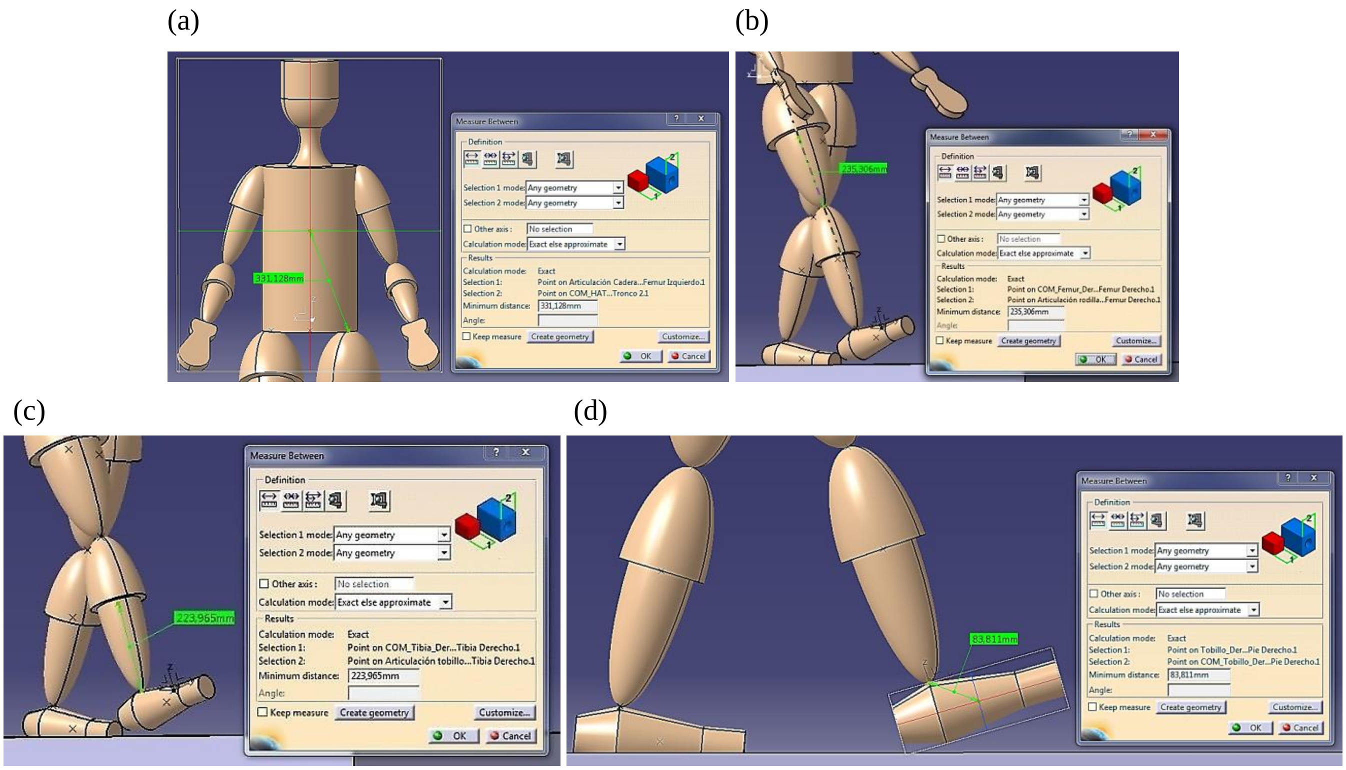

Fig. 10 COM positions in the lower segments, phase: left support and right swing – virtual mannequin. (a) COM position in HAT - left hip in support, (b) COM position in the right femur, (c) COM position in the right tibia, and (d) COM position on right foot in the swing phase

- ***Moments of inertia:*** The mass distribution in human segments changes during walking. Table 13 presents the values of the moments of inertia for the COMs of the lower limbs in the double support phase, and Fig. 11 shows the selected lower segments in the exoskeleton, both, right and left sides.

Table 13 Moments of inertia passing through the COM of the segment with respect to the axis of rotation, phase: double support – virtual mannequin

Joint - Segment	$\boldsymbol{I_{axis\_COM} = I_{oxG}[Kgm^2]}$
Right ankle - Right foot	0.005
Right ankle - Tibia	0.028
Right knee - Femur	0.073
Right hip - HAT	**2.395**
Left hip - HAT	**2.395**
Left knee- Femur	0.073
Left ankle - Tibia	0.028
Left ankle - Left foot	0.005

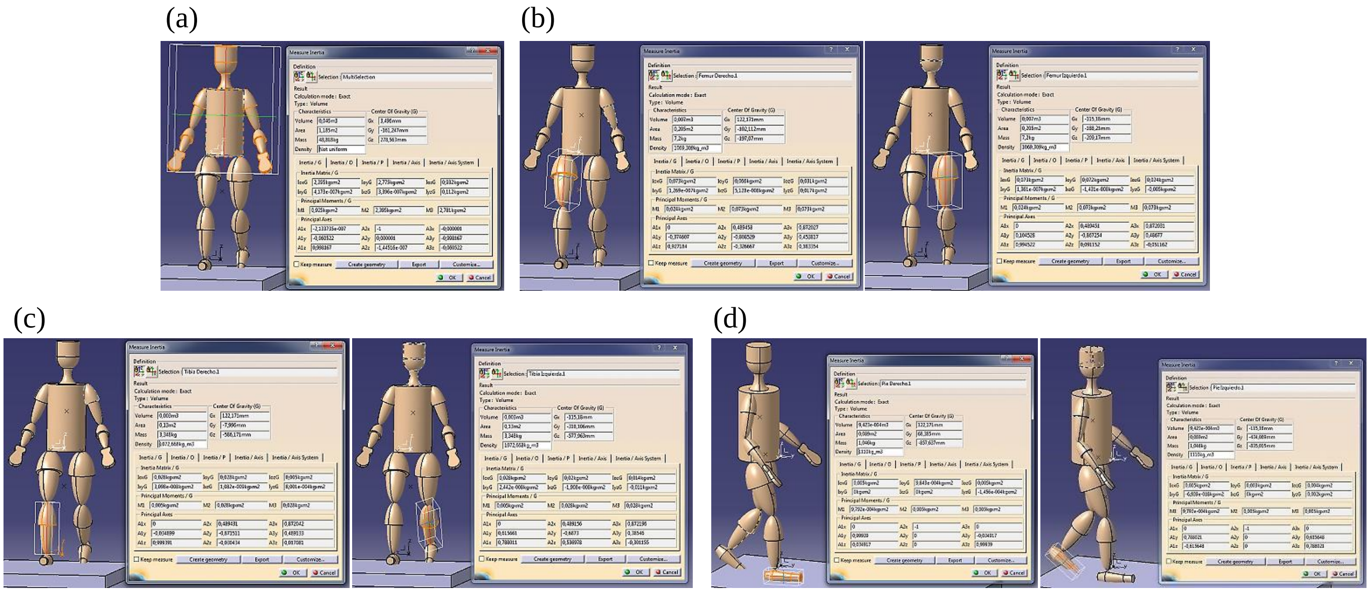

Fig. 11 Moments of inertia in the lower limb joints, phase: double support – virtual mannequin. (a) Right and left hip in support, (b) Right and left knee in support, (c) Right and left ankle in support, (d) Right and left foot in support

The moments of inertia in the COMs for the right support-left swing phase are detailed in Table 14. The moments of inertia of the right segments in single support are the same as in the double support phase, Fig. 11(b-d, Column 1), except for the right hip - HAT segment, Fig. 12(a).

Table 14 Moments of inertia passing through the COM of the segment with respect to the axis of rotation, phase: right support and left swing - virtual mannequin

Joint - Segment	$\boldsymbol{I_{axis\_COM} = I_{oxG}[Kgm^2]}$
Right ankle - Right foot	0.005
Right ankle - Tibia	0.028
Right knee - Femur	0.073
Right hip - HAT	**2.395**
Left hip - Femur	0.073
Left knee - Tibia	0.028
Left ankle - Left foot	0.005

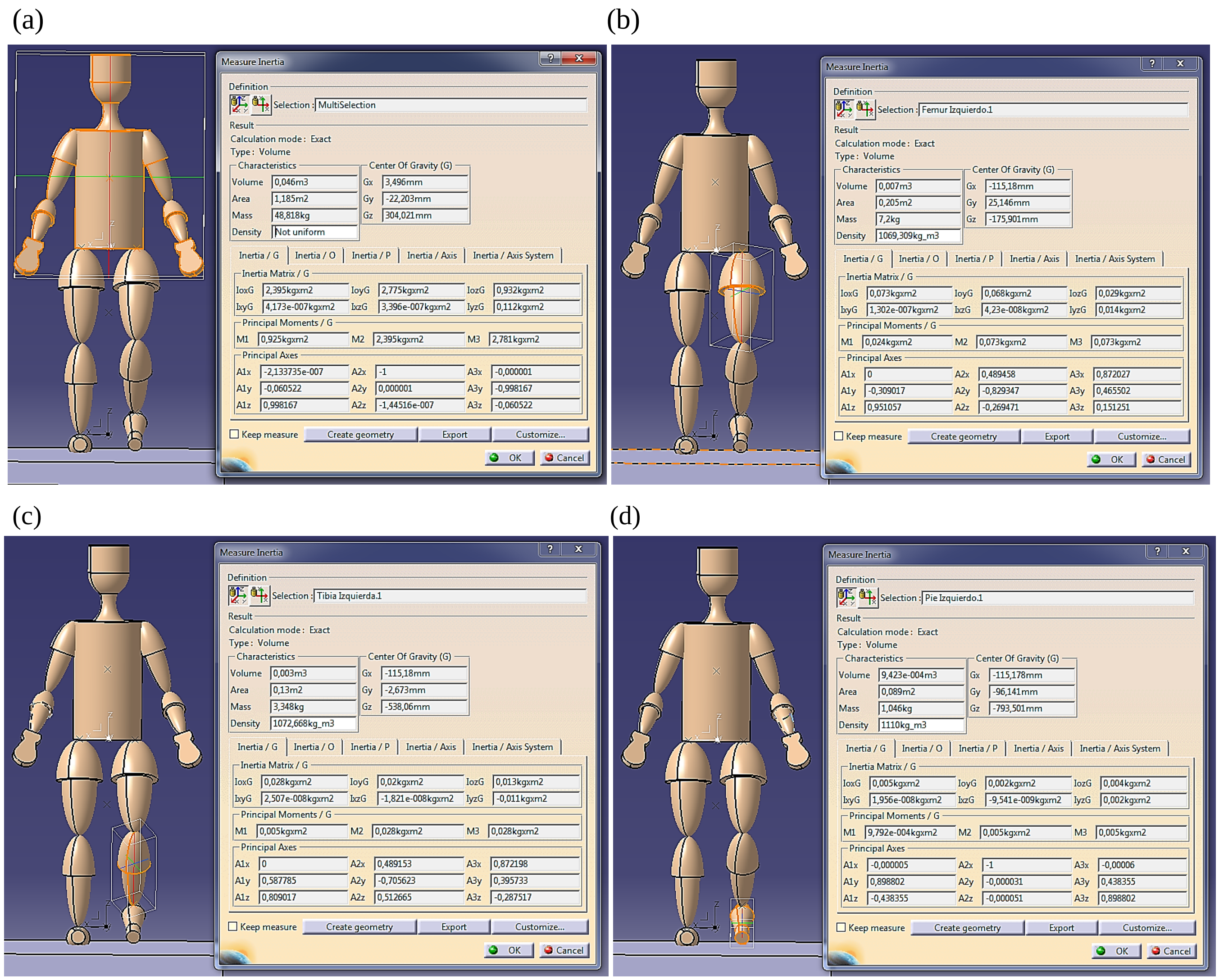

Fig. 12 Moments of inertia in the lower limb joints, phase: right support and left swing – virtual mannequin. (a) Right hip in support, (b) Left hip swing, (c) Left knee swing, (d) Left ankle swing

The moments of inertia in the positions of the COMs for the left support-right swing phase are specified in Table 15. Likewise, the moments of inertia of the left segments in single support are the same as in the double support phase, Fig. 11(b-d, Column 2), except for the left hip - HAT segment, Fig. 13(a).

Table 15 Moments of inertia passing through the COM of the segment with respect to the axis of rotation, phase: left support and right swing – virtual mannequin

Joint - Segment	$I_{axis\_COM} = I_{oxG}[Kgm^2]$
Right ankle - Right foot	0.005
Right knee - Tibia	0.028
Right hip - Femur	0.073
Left hip - HAT	**2.395**
Left knee- Femur	0.073
Left ankle - Tibia	0.028
Left ankle - Left foot	0.005

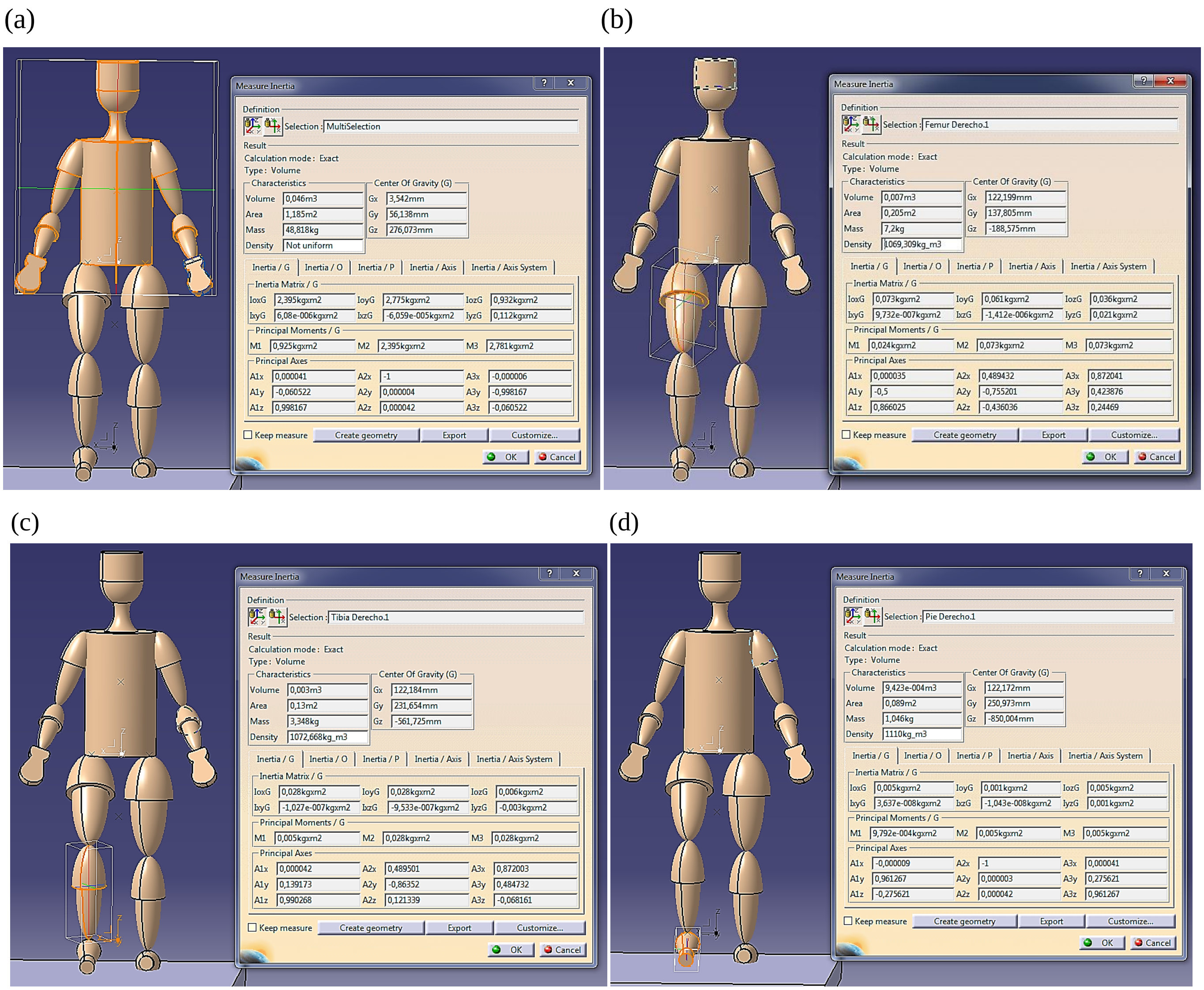

Fig. 13 Moments of inertia in the lower limb joints, phase: left support and right swing – virtual mannequin. (a) left hip in support, (b) right hip swing, (c) right knee swing, (d) right ankle swing

1.3 Mannequin + RUVEM exoskeleton

This section details the physical parameters of the mannequin wearing the RUVEM lower limb exoskeleton, Fig. 1(c), which are to parameterize the dynamic model of the human–exoskeleton system. These parameters comprise the COM locations for each lower-limb segment, along with the associated moments of inertia computed about the respective COMs. Together, these values establish the basis for accurately modeling the dynamic behavior of the human-exoskeleton during motion and for subsequent analysis of its interaction with the human user.

- ***Positions of the COMs:*** The mass distribution in each segment changes during the gait cycle; therefore, the position of the COM in each segment also changes. Table 16 shows the masses of the exoskeleton segments without the motors.

Table 16 Mass of mannequin-exoskeleton segments without motors

Right/left segment	Mass $[Kg]$
Foot	1.235
Tibia	4.531
Femur	8.595
HAT	50.396

For the double support phase, Table 17 presents the distal distances between the segment joints and the corresponding positions of the COMs. In addition, Fig. 14 illustrates the COM locations in the right and left lower-limb segments with respect to each joint.

Table 17 COM's positions in the lower segments, phase: double support – Mannequin wearing the RUVEM Exoskeleton with motors

Segment	Distal distance $[m]$
Right foot - Ankle	-
Right tibia - Ankle	0.309391
Right femur - Knee	0.294682
HAT - Right hip	0.324614
HAT - Middle hip	**0.302253**
HAT - Left hip	0.324819
Left foot - Ankle	-
Left tibia - Ankle	0.309574
Left femur - Knee	0.291707

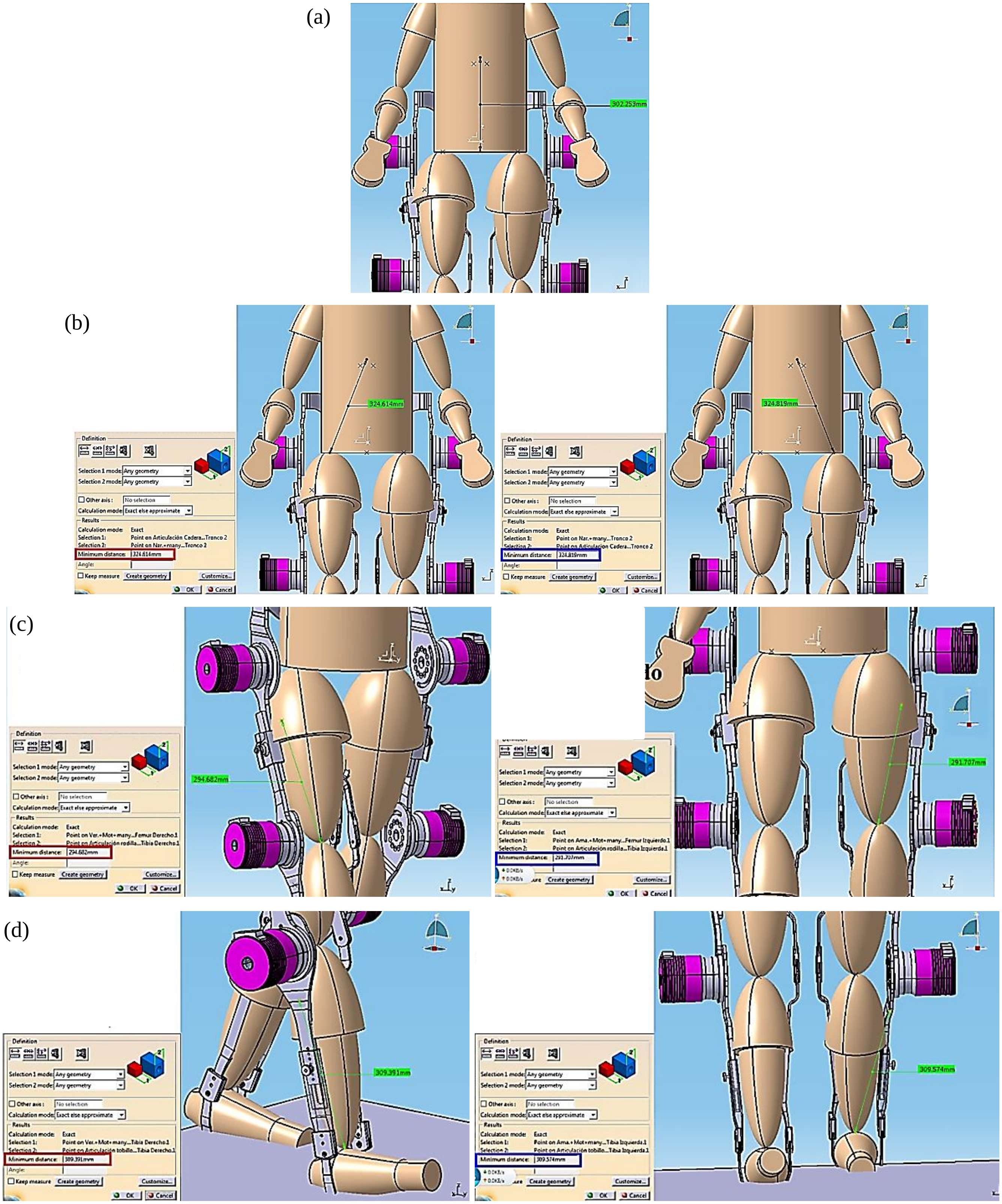

Fig. 14 COM positions in the lower limb segments during the double-support phase of the Mannequin+RUVEM Exoskeleton with motors: (a) Hip at the center, (b) COM position in the HAT with right and left hip, (c) COM position in the right and left femur, and (d) COM position in the right and left tibia

For the right support and left swing phase, Fig. 15 and Table 18 present the distal distances between the joints of the corresponding segments and the positions of the COMs. The segments of the right limb remain unchanged. In the mathematical model, it is assumed that the distance between either hip joint and the COM position in the HAT segment remains constant throughout the gait cycle. Additionally, for the swing segment, the proximal COM distance is used, which is obtained as the difference between the total segment length and the distal COM distance.

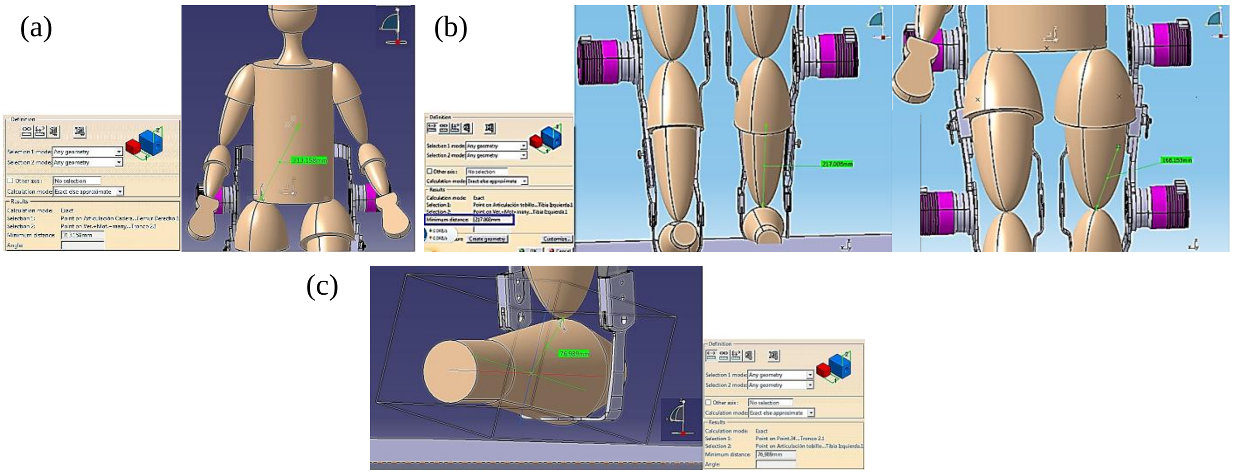

Fig. 15 COM positions in the lower segments, phase: right support/left swing – Mannequin+RUVEM Exoskeleton with motors. (a) COM position in HAT - right hip in support, (b) COM position in the left tibia and left femur, both in a swing phase, and (c) COM position on left foot in the swing phase

Table 18 COM's positions in the lower segments, phase: right support and left swing - Mannequin wearing the RUVEM Exoskeleton with motors

Segment	**Distal distance** $[m]$
Right foot - Ankle	-
Right tibia - Ankle	0.309391
Right femur - Knee	0.294682
HAT - Right hip	**0.313158**
Left foot - Ankle	0,076989
Left tibia - Ankle	0.217008
Left femur - Knee	0.168153

For the left support and right swing phase, Table 19 and Fig. 16 present the distal distances between the joints and the corresponding positions of the centers of mass (COMs). The values for the segments of the left limb remain the same as those used in the double support phase.

Table 19 COM's positions in the lower segments, phase: left support and right swing - Mannequin wearing the RUVEM Exoskeleton with motors

Segment	**Distal distance** $[m]$
Right foot - Ankle	0,076989
Right tibia - Ankle	0.21669
Right femur - Knee	0.168741
HAT - Left hip	**0.313396**
Left foot - Ankle	-
Left tibia - Ankle	0.309574
Left femur - Knee	0.291707

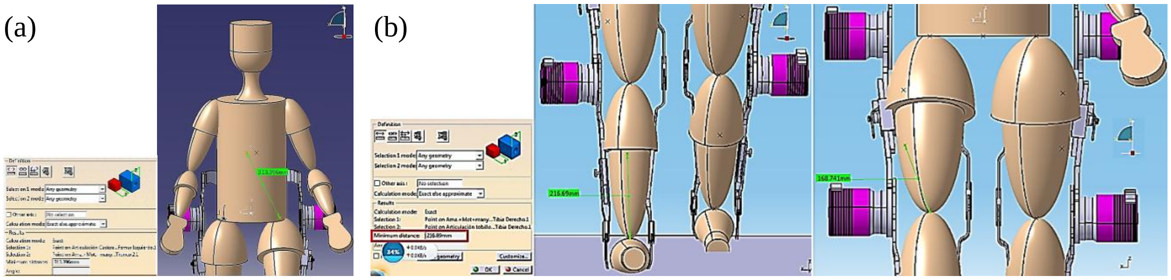

Fig. 16 COM positions in the lower segments, phase: left support and right swing – Mannequin+RUVEM Exoskeleton. (a) COM position in HAT - left hip in support, and (b) COM position in the right tibia and right femur, both in a swing phase

- ***Moments of inertia:*** For each joint and segment, this parameter varies depending on the current phase of the gait cycle. During the double support phase, Table 20 presents the moments of inertia calculated about the COMs of the lower-limb segments. In addition, Fig. 17 illustrates the selected exoskeleton segments, on both the right and left sides, used to estimate these moments of inertia.

Table 20 Moments of inertia passing through the COM of the segment with respect to the axis of rotation, phase: double support - Mannequin wearing the RUVEM Exoskeleton

Joint – Segment	$\boldsymbol{I_{axis\_COM} = I_{oxG}[Kgm^2]}$
Right ankle - Right foot	0.013
Right ankle - Tibia	0.0770
Right knee - Femur	0.1430
Right hip - HAT	**1.7797**
Left hip - HAT	**1.7797**
Left knee- Femur	0.1708
Left ankle - Tibia	0.0770
Left ankle - Left foot	0.013

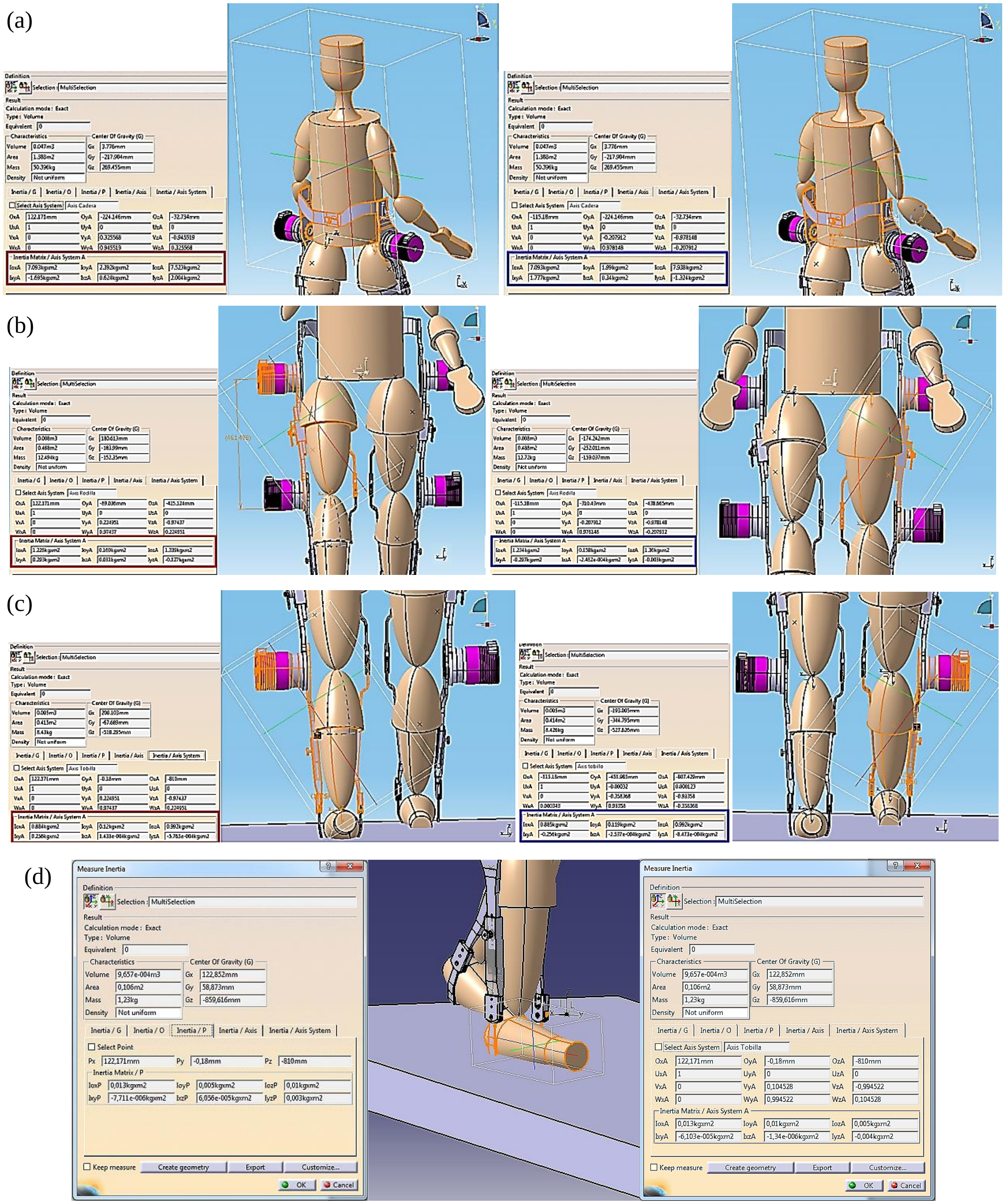

Fig. 17 Moments of inertia in the COMs of the lower segments, phase: double support – Mannequin+RUVEM Exoskeleton. (a) Right and left hip in support, (b) Right and left knee in support, (c) Right and left ankle in support, (d) Right and left foot in support

The moments of inertia about the COMs of the lower-limb segments for the right support–left swing phase are presented in Table 21 and Fig. 18. For the right limb segments in single support, the moments of inertia remain the same as in the double support phase, Fig. 17(b–d, Column 1), except for the right hip–HAT segment, as shown in Fig. 18(a).

Table 21 Moments of inertia passing through the COM of the segment with respect to the axis of rotation, phase: right support and left swing - Mannequin wearing the RUVEM Exoskeleton

Joint - Segment	$I_{axis\_COM} = I_{oxG}[Kgm^2]$
Right ankle - Right foot	0.013
Right ankle - Tibia	0.0770
Right knee - Femur	0.1430
Right hip - HAT	**1.7733**
Left hip - Femur	0.3166
Left knee - Tibia	0.0555
Left ankle - Left foot	0.0050

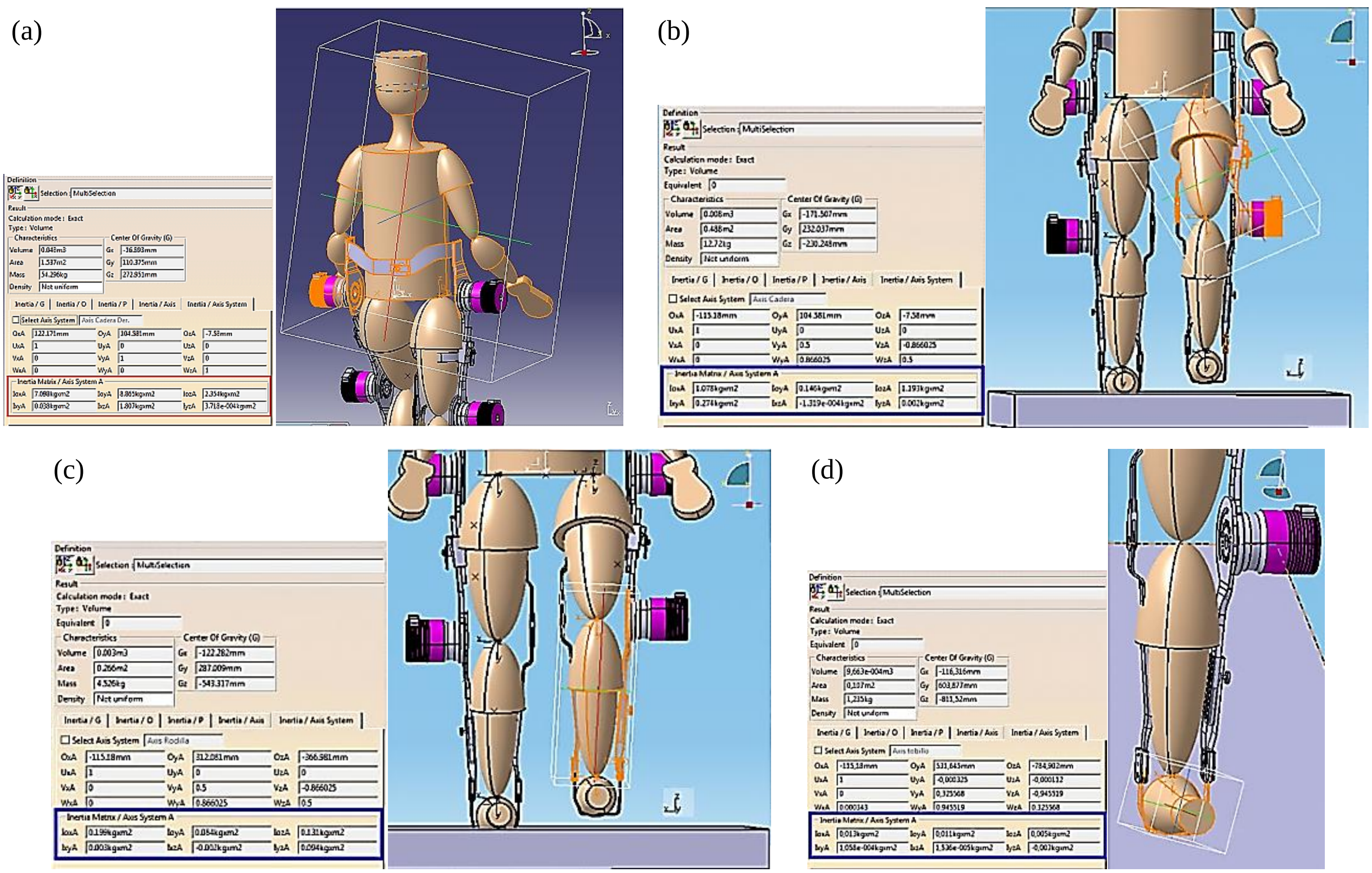

Fig. 18 Moments of inertia in the COMs of the lower segments, phase: right support and left swing – Mannequin+RUVEM Exoskeleton. (a) Right hip in support, (b) Left hip swing, (c) Left knee swing, and (d) Left ankle swing

The moments of inertia about the COMs of the segments for the left support–right swing phase are presented in Table 22 and Fig. 19. Similarly, for the left limb segments in single support, the moments of inertia remain the same as in the double support phase Fig. 17(b–d, Column 2), except for the left hip–HAT segment, as illustrated in Fig. 19.

Table 22 Moments of inertia passing through the COM of the segment with respect to the axis of rotation, phase: left support and right swing - Mannequin wearing the RUVEM Exoskeleton

Joint - Segment	$I_{axis\_COM} = I_{oxG}[Kgm^2]$
Right ankle - Right foot	0.0050
Right knee - Tibia	0.0559
Right hip - Femur	0.2973
Left hip - HAT	**1.7652**
Left knee- Femur	0.1708
Left ankle - Tibia	0.0770
Left ankle - Left foot	0.013

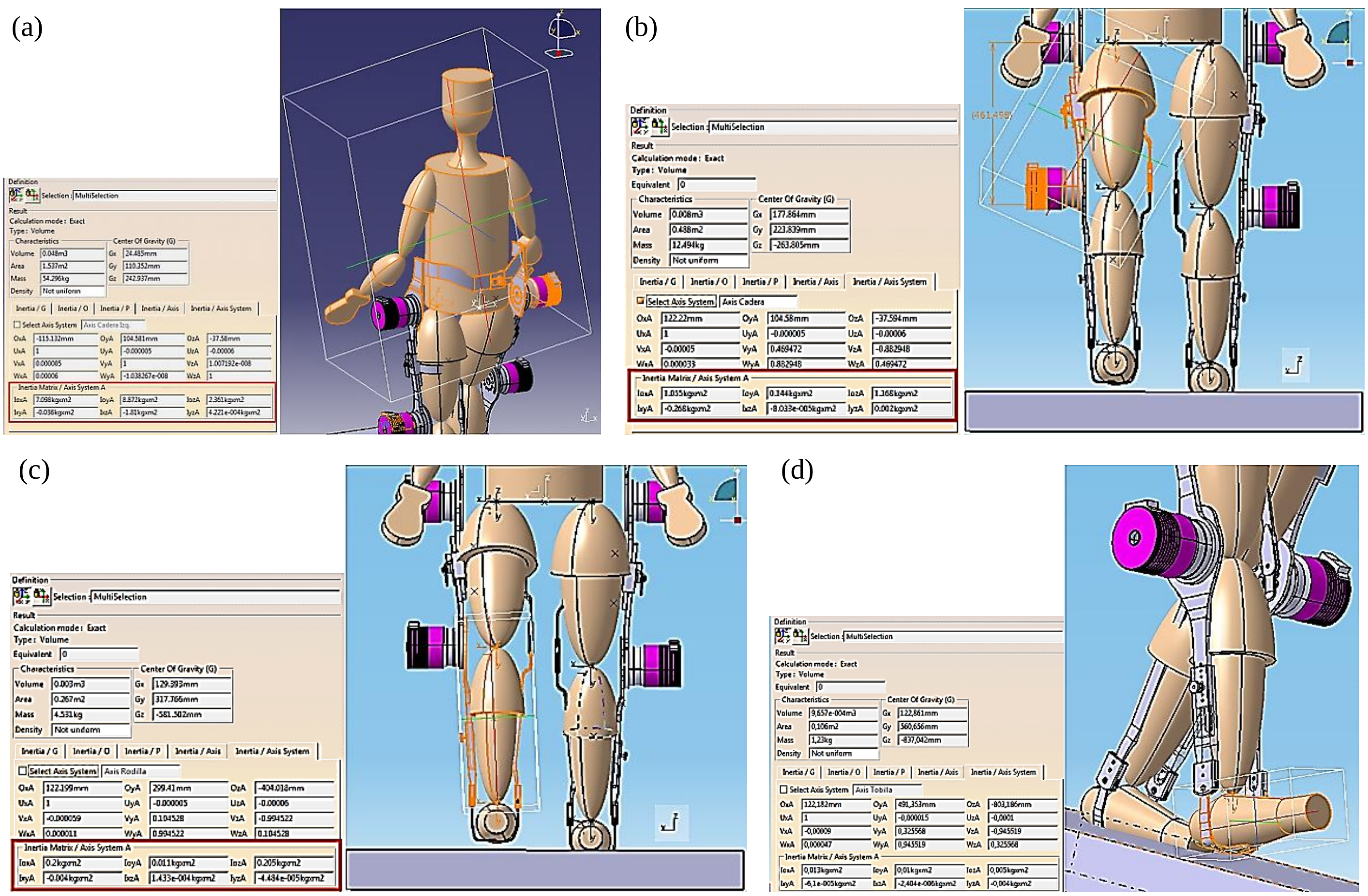

Fig. 19 Moments of inertia in the COMs of the lower segments, phase: left support and right swing – Mannequin+RUVEM Exoskeleton. (a) Left hip in support, (b) Right hip swing, (c) Right knee swing, (d) Right ankle swing

1.4 RUVEM Actuator

The RUVEM exoskeleton has servomotors in the knees and hips [7], and the ankle joints are under-actuated. The characteristic parameters of the servomotor are described in Fig. 20(a) and Table 23. The servomotor is shown in Fig. 20(b); it has a built-in brake, which is deactivated with 24 Vdc.

(a)

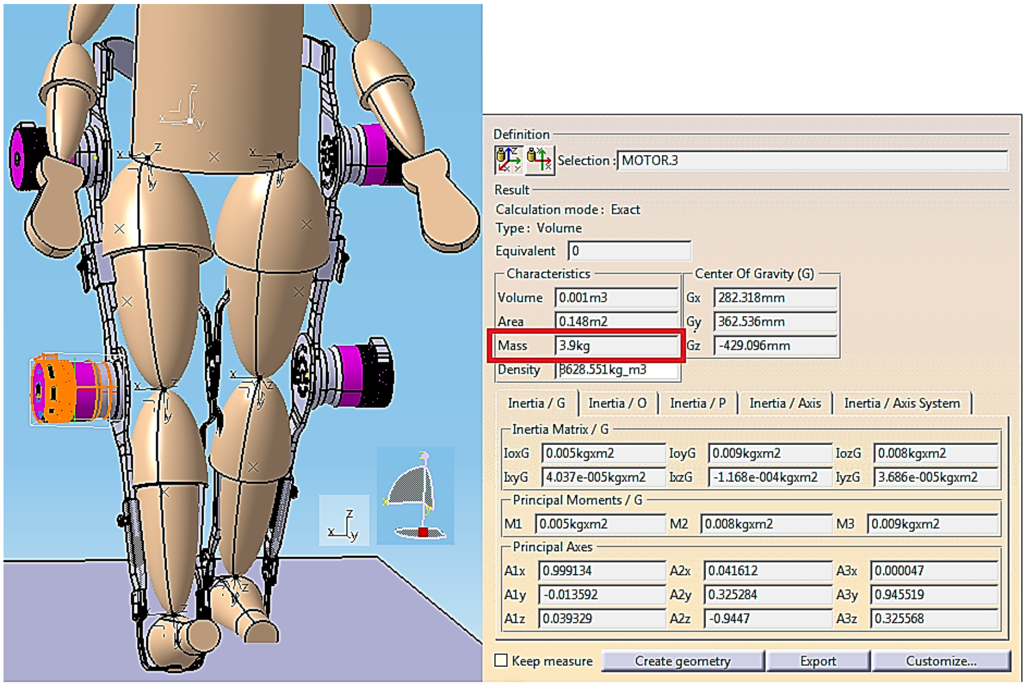

(b)

Fig. 20 (a) Servomotor coupled to the exoskeleton, and (b) Servomotor [7]

Table 23 Parameters of the Harmonic Drive AG servomotor with built-in brake

Parameter	Value
Mass	3.9 Kg
Maximum torque	82 Nm
Maximum current	2.8 A_{rms}
Torque constant	33.4 Nm/A
Terminal voltage 3ϕ (L-L)	220 V_{rms}
Moment of inertia at the output (motor with brake)	0.000139 Kgm^2
Maximum speed	60 rpm
Motor armature resistance (L-L, 20 °C)	5.9 Ω
Motor armature inductance (L-L, 20 °C)	8.0 mH
AC voltage constant (L-L, 20° C, at motor)	23 $V_{rms}/1000\ rpm$

2. Case study: Exo-H3 exoskeleton

The virtual model of the Exo-H3 exoskeleton is contained in a URDF file (Unified Robot Description Format) with the description of the inertial properties obtained from the mechanical design, it also contains the links to the visual and collision meshes, Fig. 21(a). For simulation purposes, the model allows the choice of different sizes to fit different human anthropometries. The parameters such as the COM positions in the segments and the moments of inertia in the COMs are presented for two healthy subjects.

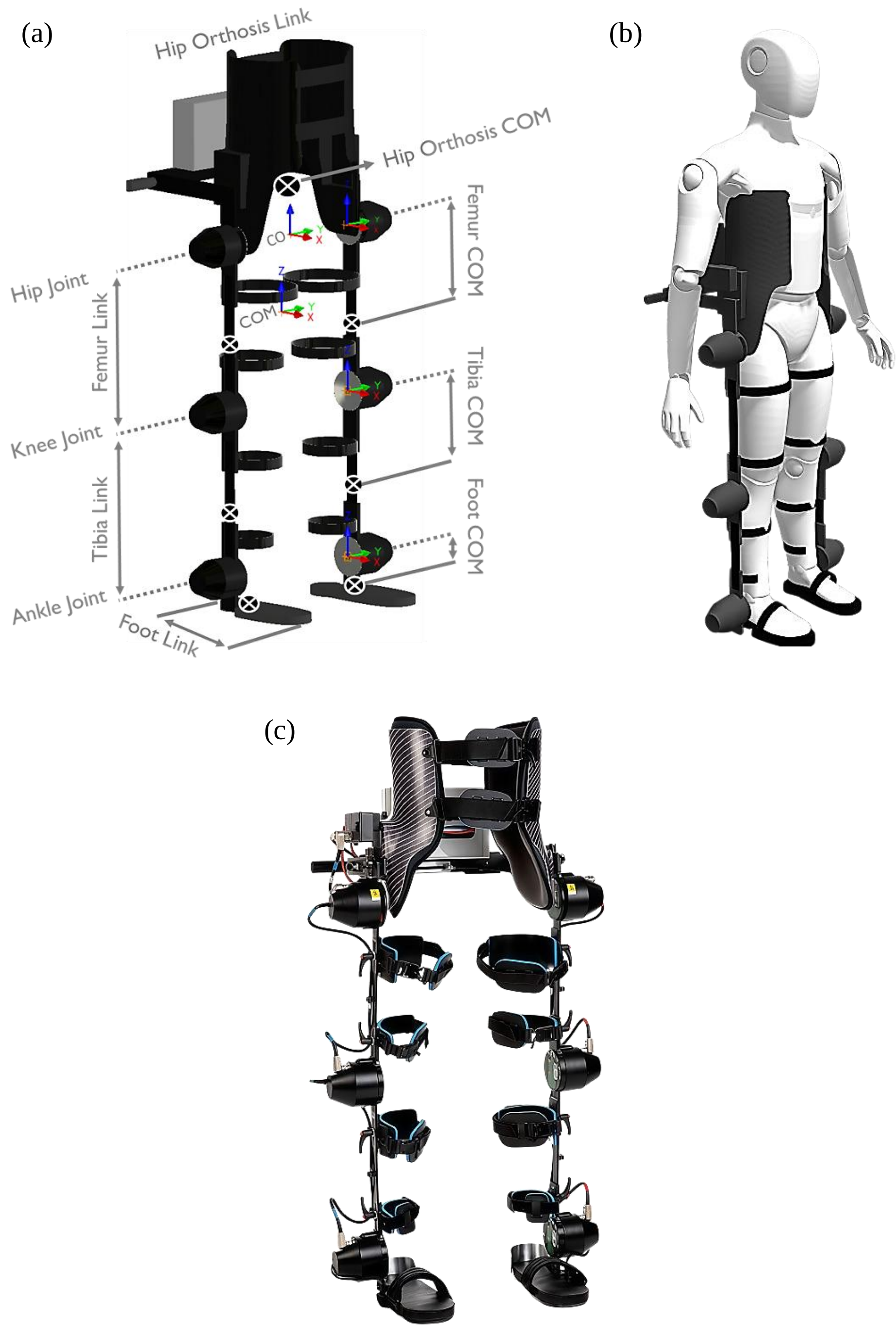

Fig. 21 Exo-H3 Exoskeleton. (a) Coordinate frame of the CAD model for the Exo-H3 exoskeleton, (b) Virtual Mannequin-Exo-H3 exoskeleton, and (c) Exo-H3 lower limb exoskeleton owned by Technaid S.L. [8]

2.1 Subject + Exo-H3 Lower limb exoskeleton

This section details the physical parameters of the Exo-H3 lower limb exoskeleton Fig. 21(c), which are necessary to parameterize its dynamic representation. The parameters include the positions of the COMs for each segment, the corresponding moments of inertia about the COMs, and the anthropometric data of the human user. Together, these parameters provide the basis for modeling the coupled dynamics of the Exo-H3 and the human body, Fig. 21(b).

- ***Positions of the COMs:*** The coordinate frame origin of the total assembly and the hip link is in the middle of the line parallel to the $\boldsymbol{y}$-axis between hip joints, Fig. 21(a); and for each link, the coordinate frame origin is in the axis of rotation, $\boldsymbol{y}$-axis, of the joint. The masses of the exoskeleton segments with servomotors are indicated in Table 24, and the COM positions for each adjustment in the exoskeleton according to the subjects are listed in Table 25.

Table 24 Mass of exoskeleton segments with servomotors

Right/left segment	**Mass [$\boldsymbol{Kg}$]**
Foot	0.909
Tibia	1.647
Femur	1.715
Trunk (with battery)	7.043

Table 25 COM positions in the exoskeleton segments with servomotors

Subject	**Joint – Segment's COM**	**Right limb Distal distance [$\boldsymbol{m}$]**	**Left limb Distal distance [$\boldsymbol{m}$]**
01	Ankle joint to the COM of the foot	0.0538650	0.0538555
	Knee joint to the COM of the tibia	0.2817483	0.2817459
	Hip joint to the COM of the femur	0.2742621	0.2742622
	Hip joint to the COM of the trunk (width:4 depth:6) with battery	0.2516053	0.2731002
	Center point between hips to the COM of the trunk (width: 4 depth: 6) with battery	0.1697452	
	Hip joint to the COM of the trunk (width: 4 depth: 6) without battery	0.2068981	0.2539727
	Center point between hips to the COM of the trunk (width: 4 depth: 6) without battery	0.1164021	
02	Ankle joint to the COM of the foot	0.0538650	0.0538555
	Knee joint to the COM of the tibia	0.2528924	0.2528906
	Hip joint to the COM of the femur	0.2456297	0.2456322
	Hip joint to the COM of the trunk (width: 4 depth: 6) with battery	0.2516053	0.2731002
	Center point between hips to the COM of the trunk (width: 4 depth: 6) with battery	0.1697452	
	Hip joint to the COM of the trunk (width: 4 depth: 6) without battery	0.2068981	0.2539727
	Center point between hips to the COM of the trunk (width: 4 depth: 6) without battery	0.1164021	

- ***Human anthropometry:*** Table 26 summarizes the anthropometric data of two healthy subjects.

Table 26 Anthropometric data from healthy subjects

Anthropometric data	Subject 01	Subject 02
Mass $[kg]$	82.900	67.100
Height $[m]$	1.850	1.660
Right femur (greater trochanter-lateral tibial $[m]$	0.490	0.415
Right tibia (medial tibial- medial malleolus) $[m]$	0.400	0.360
Right foot (acropodion - pternion) $[m]$	0.290	0.260
Left femur $[m]$	0.485	0.415
Left tibia $[m]$	0.400	0.360
Left foot $[m]$	0.290	0.260

- ***Moments of inertia:*** This parameter is calculated concerning the COM. The moment of inertia for each adjustment in the exoskeleton according to subjects is shown in Table 27.

Table 27 Moments of inertia through COM of the segment according to the rotation axis; exoskeleton with servomotors

Subject	Joint – Segment	Right limb Inertia tensor $[Kgm^2]$	Left limb Inertia tensor $[Kgm^2]$
		I_{yy}	I_{yy}
01	Ankle joint – Foot	0.005194850	0.005194980
	Knee joint – Tibia	0.063655600	0.063650300
	Hip joint – Femur	0.067669400	0.067632300
	Hip joint – Trunk (width: 4 depth: 6) with battery	0.146913319	
	Hip joint – Trunk (width: 4 depth: 6) without battery	0.093884201	
02	Ankle joint - Foot	0.005194850	0.005194980
	Knee joint - Tibia	0.050175700	0.050170400
	Hip joint - Femur	0.053607600	0.053571300
	Hip joint – Trunk (width: 4 depth: 6) with battery	0.146913319	
	Hip joint – Trunk (width: 4 depth: 6) without battery	0.093884201	

2.2 Exo-H3 Actuator

The joints of Exo-H3 exoskeleton are driven by DC brushless Maxon motors coupled with harmonic drive units [8], Fig. 22(a-c). The motor, gearbox, battery and exoskeleton data are summarized in Table 28.

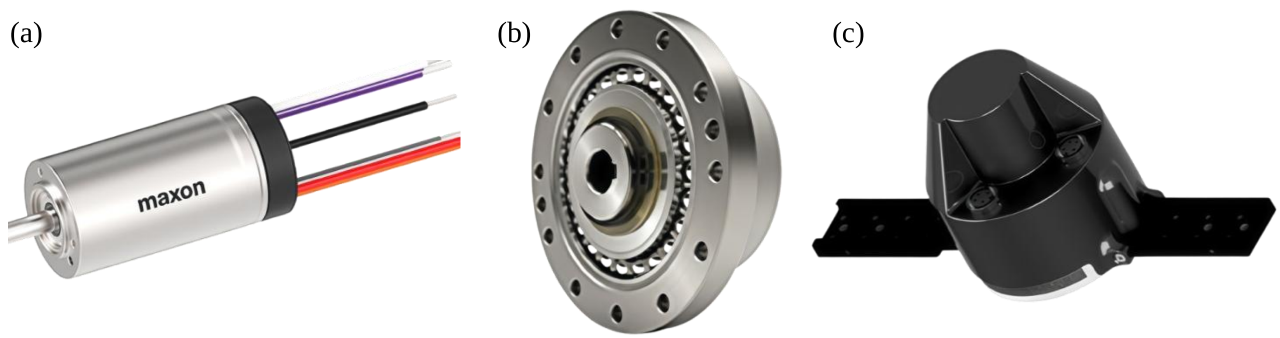

Fig. 22 Exo-H3's actuation system. (a) BLDC motor from Maxon [9], (b) Harmonic Drive gearbox [10], and (c) Powered exoskeleton joint [8]

Table 28 Technical specifications for motor, gearbox, battery, and exoskeleton

	Parameter	Value
Motor	Nominal speed	410.5 rad/s (3920 rpm)
	Nominal voltage	18 V
	Nominal current (max. continuous current)	5.46 A
	Nominal torque (max. continuous torque)	$207x10^{-3}$ Nm
	Nominal power	100 W
	No load speed	4550 rpm
	No load current	$352x10^{-3}$ A
	Stopping torque	3.26 Nm
	Starting current	87 A
	Rotor inertia	$4.4x10^{-6}$ Kgm^2
	Motor weight	0.390 Kg
	Terminal resistance phase to phase	0.236 Ω
	Terminal inductance phase to phase	$169x10^{-6}$ H
	Torque constant	$37.5x10^{-6}$ Nm/A
	Speed constant	26.7 $rad/s/V$ (255 rpm/V)
	Speed/torque gradient	1410 rpm/Nm
	Mechanical time constant	$0.648x10^{-3}$ s
Gearbox	Gearbox ratio	160
	Weight of the gearbox	0.24 Kg
	Moment of inertia at the gearbox input	$28.2x10^{-6}$ Kgm^2
	Backdriving torque without load of gearbox	12 Nm
Battery $LiFePO_4$	Weight	2.388 Kg
	Normal capacity type	10.8 Ah
	Normal voltage	19.2Vdc
	Normal energy	*230 Wh*
	Standard discharge current (const.)	2.4 A
Exoskeleton	Net joint torque	35 Nm
	Peak joint torque	152 Nm
	Dimensions (tall/long/wide)	118/45/30 cm
	Weight (with/without battery)	17/14.2 Kg

3. References

1. González-Mejía S (2023) Partial Assistance Control on a Robotic Platform with an Exoskeleton for the Human Gait Rehabilitation. Doctoral thesis, Universidad del Valle, Cali, Colombia
2. Dassault Systèmes (2025) Software CAD 3D | CATIA. https://www.3ds.com/es/products/catia. Accessed 9 Sep 2025
3. Dassault Systèmes (2025) Software de operaciones globales | DELMIA. https://www.3ds.com/es/products/delmia/. Accessed 9 Sep 2025
4. Winter DA (2009) Biomechanics and motor control of human movement, Fourth Edi. Hoboken, New Jersey
5. GICI (2026) Industrial Control Research Group - Universidad del Valle. https://gici.univalle.edu.co/. Accessed 1 Feb 2026
6. Landau DL, Lifshitz EM, Berestetskii VB, Pitaevskii LP (1970) Física Teórica, Mecánica, 2nd ed. Moscou
7. Harmonic Drive AG (2025) CHA Servo actuator with hollow shaft. https://harmonicdrive.de/en/product/actuators-with-hollow-shaft/cha. Accessed 23 Oct 2025
8. Technaid - Leading Motion (2026) Robotic Exoskeleton Exo-H3. https://www.technaid.com/products/robotic-exoskeleton-exo-exoesqueleto-h3/. Accessed 20 Mar 2026
9. Maxon (2025) BLDC motors with ironless or iron core winding. https://www.maxongroup.com/en/drives-and-systems/brushless-dc-motors. Accessed 23 Oct 2025
10. Harmonic Drive (2025) Gear Units. https://www.harmonicdrive.net/products/gear-units. Accessed 23 Oct 2025